Am J Transl Res 2019;11(10):6585-6599
www.ajtr.org /ISSN:1943-8141/AJTR0102651

Original Article

Pituitary adenylate cyclase-activating polypeptide ameliorates radiation-induced cardiac injury

Huan Li[1*], Lu Cao[1*], Pei-Qiang Yi[1], Cheng Xu[1], Jun Su[1], Pei-Zhan Chen[2], Min Li[1], Jia-Yi Chen[1]

[1]Department of Radiation Oncology, Ruijin Hospital, Shanghai Jiaotong University School of Medicine, Shanghai, China; [2]Clinical Research Center, Ruijin Hospital North, Shanghai Jiaotong University School of Medicine, Shanghai, China. [*]Equal contributors.

Received September 23, 2019; Accepted October 11, 2019; Epub October 15, 2019; Published October 30, 2019

Abstract: Radiation-induced heart disease (RIHD) is a common sequelae of thoracic irradiation. Currently, there is no effective prevention and treatment strategy. Oxidative stress is associated with the development of RIHD. Pituitary adenylate cyclase-activating polypeptide 38 (PACAP38) has been defined as the multipotent properties of cytoprotective effect on its anti-apoptotic and antioxidant activities. Here, we set to investigate whether PACAP38 plays a role in attenuating RIHD. We established radiation-related cardiac injury models using 6MV X-ray based on H9C2 cardiomyocytes and male C57/BL6 mice which were pre-treated with PACAP38 prior to radiation exposure. PACAP38 protected mice from radiation-induced histological damage including myocardial apoptosis and fibrosis. Also, cell viability and colony-forming efficiency were enhanced and intracellular ROS generation was reduced in PACAP38 treated H9C2 cardiomyocytes exposed to radiation. Moreover, PACAP38 suppressed myocardial apoptosis and G2/M arrest through blunting the radiation-induced down-regulation of Bcl-2, CyclinB1 and CDC2, and inhibiting the up-regulation of Bax. Furthermore, irradiation resulted in activating of NRF2 and HO-1 expressions were further enhanced by PACAP38 in H9C2 cells and the protective effect of PACAP38 was partially blocked by NRF2 siRNA silencing. In summary, PACAP38 has the potential to effectively protect against acute radiation-induced cardiac injury and its cardioprotective effect involves upregulation of NRF2/HO-1-dependent signaling activation.

Keywords: Radiation-induced heart disease (RIHD), radiation-induced cardiac injury, irradiation, PACAP38, NRF2

Introduction

Radiotherapy is an indispensable part of multidisciplinary treatment of malignancies. It has previously been proposed that approximately 52.3% of all oncological patients should receive radiation during the course of their illness [1]. Normal tissue injury associated with radiotherapy are clinical issues of multidisciplinary treatment for malignancies. Radiation-induced heart diseases (RIHDs) have become one of the major causes of non-neoplastic death in patients receiving thoracic irradiation, especially with old technique of radiotherapy, particular in patients with classical Hodgkin's lymphoma [2-4] and early-stage breast cancer [5-7]. The application of more sophisticated techniques has greatly decreased the dose delivered to the whole heart and its sub-structures. Nevertheless, cardiac toxicity remains a major concern when balancing target coverage and minimizing cardiac dose in delivering radiotherapy to thoracic tumors. In addition, there is increasing use of concomitant therapies, with the consequences of different combinations yet to be determined. Some patients have shown increased cardiovascular morbidity several years following the IR with acute and chronic effects of RIHDs [8]. The clinical protocol of RIHDs currently is established decades with cardiac diseases of etiology not specific to anti-cancer therapy, therefore, it is essential to define therapeutic targets during the course of RIHDs and exploit the novel agent to prevent and reduce heart injury from radiation therapy.

The cardiovascular complications of radiotherapy include coronary artery disease, pericardial disease, cardiomyopathy/myocardial fibrosis, valvular disease and arrhythmia [9]. Potential mechanisms responsible for RIHDs span a variety of biologic processes, including oxidative

stress, inflammation, and elaboration of proinflammatory and profibrogenic cytokines [10]. Tissue irradiation either damages the cell DNA directly, or forms oxygen radicals in addition to the DNA damage [11]. Nuclear factor erythroid 2-related factor 2 (NRF2) is a transcription factor that maintains cellular redox homeostasis by binding to antioxidant response elements to regulate the expression of oxidative stress related proteins, including NADPH, quinone oxidoreductase 1 (NQO1), hemoxygenase 1 (HO-1), superoxide dismutase (SOD), and glutathione S-transferase proteins (GSTs) [12]. Studies have reported that NRF2 activation may play a critical role in cardioprotection of cardiovascular diseases that are relevant to oxidative stress [13]. As well, HO-1 has revealed as a crucial defense enzyme to protect cardiomyocytes against hypoxia and reoxygenation injury [14]. It has not so far identified the effect of NRF2/HO-1 pathway in radiation-related myocardial injury.

Pituitary adenylate cyclase-activating polypeptide (PACAP), an endogenous pleiotropic peptide, is a member of the secretin/vasoactive intestinal peptide (VIP) family [15, 16]. Its 38-amino-acid form (PACAP38) has been shown to protect against oxidative stress [17] and doxorubicin [18] induced apoptotic cell death in cardiomyocytes. PACAP38 inhibited the expression of pro-apoptotic factors bax and c-Jun through PI3K/Akt pathway [19] and alleviated doxorubicin-induced cardiomyopathy in PACAP knockout mice [20]. PACAP38 has emerged potent cytoprotective roles based on its anti-inflammatory, anti-apoptotic and antioxidant activities. In the present study, we have shown the efficacy of PACAP38 as a cardioprotectant both in vivo and in vitro, which could provide the rationale for using PACAP38 as an effective therapy for RIHDs. We also determined the central role of NRF2/HO-1 activation in radiation-induced cardiotoxicity as well as the cardioprotective mechanism of PACAP38.

Materials and methods

Irradiation and treatment in vivo

All animal experiments and procedures were performed with the approval of the Shanghai Jiaotong University School of Medicine Institutional Animal Care and Use Committee. Cardiac injury was conducted on male C57/BL6 mice (20-25 g, 6-8 weeks old). Cardiac injury model was established by exposing murine heart for X-ray irradiation. Each animal was anesthetized with an intraperitoneal injection of 0.1 ml/10 g body weight of 4% (w/v) chloral hydrate before local heart irradiation. The control group received a sham operation. The irradiation was performed on 6-MV X-ray beam energy with 14 Gy/1Fx dose and 300 cGy/min dose rate, as well as setting source-surface distance (SSD) for 100 cm and radiation field for 1 × 1 cm, by using a medical linear accelerator (Varian Trilogy, FL, USA). The IR group received irradiation followed by 21 days of follow up. The treatment groups were given PACAP38 (A1439, Sigma-Aldrich, St. Louis, MO, USA) (10 μg/100 μl) intraperitoneally (i.p.) 2 h before irradiation and additional doses were given at 24 h and 48 h after irradiation. Control mice received equal volumes of saline i.p. Heart samples were harvested on the 21st day after irradiation.

Histological evaluation

Cardiac injury and myocardial fibrosis after IR with or without PACAP38 treatment were evaluated in hematoxylin and eosin (HE)- and Masson's trichrome-stained sections, respectively. The sections were observed and photographed by two investigators who were blinded to the treatment under a microscopy (Zeiss AxioVert A1, Jena, Germany) and images were semi-quantitatively analyzed using ImageJ software (NIH, Bethesda, MD).

In situ detection of apoptosis

Apoptotic cells in the myocardium were detected *in situ* in heart sections with the terminal deoxynucleotidyl transferase mediated dUTP nick end labeling (TUNEL) assay kit (Roche, Basel, Switzerland). Heart tissue sections were deparaffinized and rehydrated, and the number of apoptotic cells in the myocardium was semi-quantitatively measured by counting 3- to 4-high-power fields (HPF, H400) per section.

Culture of rat cardiomyocytes and IR simulated in vitro

Rat embryonic ventricular derived H9C2 cardiomyoblasts cells were purchased from the ATCC (CRL-1446, Rockville, MD, USA). The cells were cultured in DMEM (Hyclone, Logan, UT, USA) supplemented with 10% FBS (Gibco, NY, USA),

100 μg/ml streptomycin, and 100 units/ml penicillin at 37°C in a humidified incubator with an atmosphere of 95% air and 5% CO_2. The cells were irradiated using a medical linear accelerator (Varian Trilogy, FL, USA) with beam energy at 6-MV X-rays, dose rate at 300 cGy/min; source-surface distance (SSD) at 100 cm and radiation field at 30 × 30 cm with 1 cm solid water build-up and 5 cm solid water backscatter. PACAP38 was purchased from Sigma-Aldrich (A1439, St. Louis, MO, USA). The cells were pre-treated with PACAP38 (10^{-7} M or 10^{-9} M) two hours before exposure to radiation at the dose of 12 Gy.

Cell viability and clone formation assays

Cell viability was examined by CCK-8 assay (Beyotime, Shanghai, China). H9C2 cells were inoculated in 96-well culture plates overnight, then pre-treated with PACAP38 (10^{-7} M or 10^{-9} M) 2 h before exposure to IR at dose of 12 Gy. At 48 h after IR, the cells were assayed for cell viability in a humidified incubator at 37°C according to the manufacturer's instructions. The optical density was measured at 450 nm with a microplate reader (Synergy 2, BioTek, Winooski, VT, USA).

The effect of PACAP38 on the radiosensitivity of H9C2 cells at various irradiation doses (0, 2, 4, 8 Gy) was determined by clone formation assay. The cells were inoculated into cell culture plates at a density of 500-8000 cells/dish varied with the IR doses. After treatments, the cells were further cultured for 14 days and fixed and stained with crystal violet. Colonies containing more than 50 cells were counted.

Detection of reactive oxygen species (ROS)

Intracellular ROS level was detected by a Reactive Oxygen Species Assay Kit (Beyotime Biotechnology, Shanghai, China). Briefly, H9C2 cells were incubated with 1 μM of 2,7-dichlordihydrofluorescein diacetate (DCFH-DA) at 37°C for 30 min in 6-well culture plates after treatments for 48 h. DCF fluorescence intensity was observed under fluorescence microscopy (Zeiss AxioVert A1, Jena, Germany) and quantitated using the ImageJ software (NIH, Bethesda, MD).

Cell apoptosis and cell cycles analysis

Apoptosis in cell cultures was quantified with flow cytometry by staining cells with FITC-labeled annexin V and propidium iodide (PI) (Invitrogen, Carlsbad, CA, USA). Briefly, at 48 h after simulated IR and/or pre-treatment with PACAP38, H9C2 cardiomyocytes were trypsinized from confluent monolayer cultures, washed, and resuspended in annexin V binding buffer. Cells (approx. 5×10^4 cells/ml) were incubated with FITC-labeled annexin V and PI, and analyzed in a BD FACS Aria III flow cytometer (BD Biosciences, San Jose, CA, USA).

Cell cycle analysis was performed by PI/RNase staining (BD Biosciences, San Jose, CA, USA). H9C2 myocardial cells were treated with PACAP38 for 2 hrs and irradiated at a dose of 12 Gy. Forty-eight hours after IR, all cells were collected and resuspended in 75% ethanol at 4°C overnight to fix and permeabilize. Subsequently, the cells were harvested and incubated in PI/RNase staining buffer for 15 min in the dark at room temperature. The cell samples were analyzed by flow cytometry (BD FACS Aria III) to determine the cell cycle distribution.

RNA extraction and quantitative RT-PCR

H9C2 cells were seeded into 6-well culture plates at a density of 1×10^5 cells/well. 48 h after various treatments, total RNA was isolated and extracted using TRIZOL reagent (Invitrogen, Carlsbad, CA, USA). 1 μg of total RNA was converted to the corresponding cDNA with ReverTra Ace® qPCR RT Kit (Toyobo, Osaka, Japan) and 10 ng from each sample were used for quantitative RT-PCR using the SYBR GREEN Realtime PCR Master Mix Kit (Toyobo, Osaka, Japan). The pairs of primers used for amplification of β-actin, NRF2, HO-1, Bax, Bcl2, CDC2 and CyclinB1 mRNA were synthesized based on the reported sequences (**Table 1**). The fluorescent product was detected during the annealing/extension periods, and a dissociation (melting curve) analysis was used to confirm the specificity of the amplified products on the LightCycler® 96 QPCR System (Roche, Basel, Switzerland). The relative mRNA expression was evaluated by the $2^{-\Delta\Delta Ct}$ method.

Western blot analysis

At 48 h after simulated IR and/or pre-treatment with PACAP38, H9C2 cells were harvested for western blot analysis. The cell lysates of protein (10 μg) were separated by 8-12% sodium dodecylsulfate-polyacrylamide gel electrophoresis (SDS-PAGE) and then transferred onto a

Table 1. Primers used in qRT-PCR

Primer	Sequence, 5' to 3'	
	Forward	Reverse
Nrf2	GCAACTCCAGAAGGAACAGG	GGAATGTCTCTGCCAAAAGC
β-actin	TGTTTGAGACCTTCAACACC	CGCTCATTGCCGATAGTGAT
HO-1	AGCATGTCCCAGGAT TTGTC	ACTGGGTTCTGCTTGTTTCG
Bax	CCAGGACGCATCCACCAAGAAG	GCTGCCACACGGAAGAAGACC
Bcl-2	ACGGTGGTGGAGGAACTCTTCAG	GGTGTGCAGATGCCGGTTCAG
CDC2	TGCAGGACTCCAGGCTGTATCTC	ACGAGCGAAGAATCCATGAACTGG
CyclinB1	GAGCCTGAGCCTGAACCTGTTATG	GGATCACCACCATCGTCTGCATC

polyvinylidene difluoride membrane. Western blot analysis was performed using antibodies for Bax (2772S, CST), Bcl2 (sc-7382, SANTA), CDC2 (28439S, CST), CylinB1 (4138S, CST), NRF2 (ab137550, abcam) and HO-1 (E6Z5G, CST); β-actin (4970s; CST) was used as internal control. Immunopositive blots were visualized with enhanced chemiluminescence (ECL) Kit (Beyotime Biotechnology, Shanghai, China).

siRNA transient transfection

siRNA transient transfection for NRF2 gene inhibition was used a Lipofectamine 2000 reagent (Invitrogen, Carlsbad, CA, USA). NRF2 siRNA-1, NRF2 siRNA-2 and negative-control siRNA were synthesized by GenePharma (Shanghai, China). The sequences of siRNAs were designed and synthesized as follows: NRF2 siRNA-1: sense: 5'-GAGGAUGGGAAACCUUACUTT-3', antisense 5'-AUAUUUGCAGUUGAAGGCCTT-3' and NRF2 siRNA-2: sense 5'-UUUGAGUCUAAGGAGUUCAGCUGGC-3', antisense 5'-GCCAGCUGAACUCCUUAGACUCAAA-3'. H9C2 cells were cultured for 24 h and transfected with the siRNAs. After transfection for 24 h, cells were treated with PACAP38 for 2 h before irradiation (12 Gy). 48 h after transfection with various treatment, cells were harvested and verified the expression of NRF2 and efficiency of inhibition at mRNA and proteins levels. Cell viability was performed by CCK8 assay at 48 h after irradiation as described above.

Quantifications and statistical analysis

We quantified the immunoblots using an automatic chemiluminescence image analysis system (Tanon5200, Shanghai, China) with an ImageJ analysis program (NIH, Bethesda, MD). All experiments were repeated at least 3 times, and the experimental condition was repeated in triplicate wells for each experiment. The data were presented as the means ± SEM. Unpaired Student's t-test and one-way ANOVA with Bonferroni's multiple comparison test were performed using GraphPad Prism version 5.0 c for analyses, with statistical significance set at $P < 0.05$.

Results

PACAP38 protected IR mice against myocardial injury

PACAP38-treated IR mice were protected pathologically against myocardial injury of RIHD. Representative images of the cardiac left ventricular (LV) histology from radiation exposed mice with and without PACAP38 treatment are shown in **Figure 1A** and **1B**. The pathological changes in cardiac LV sections from wild-type mice with RIHD were significantly different between the saline-treated and PACAP38-treated IR mice in both HE and Masson's trichrome stainings. IR-induced cardiac injury was characterized by cardiomyocyte degeneration, eosinophilic enhancement, cytoplasmic vacuolization, nuclear condensation and myocardial fiber contorted. PACAP38-treated IR mice showed significantly improvement on myocardial morphology (**Figure 1A**).

Mice subjected to irradiation were exerted by myocardial fibrosis including perivascular fibrosis after 21 days, which was markedly prevented by PACAP38 administration (**Figure 1B**). IR increased the area of fibrosis from 1.80 ± 0.44% (Control) to 19.10 ± 1.07% (IR) in the LV (**Figure 1C**, n = 6, $P < 0.001$ vs. sham-operated mice). In PACAP38-treated IR mice, the rise in the areas of myocardial fibrosis was markedly reduced (5.47 ± 0.41%, n = 6, $P < 0.001$). PACAP38 treatment alone showed no histological change.

The number of apoptotic cardiac cells in IR murine heart was also significantly different between saline-treated and PACAP38-treated RIHD mice (**Figure 2A**). There were 14.90 ± 0.50% apoptotic myocardium in saline-treated mice with cardiac injury vs. 1.71 ± 0.17% apoptotic myocardium in PACAP38-treated IR mice with cardiac injury ($P < 0.0001$ vs. IR alone; n = 6 per group) (**Figure 2B**).

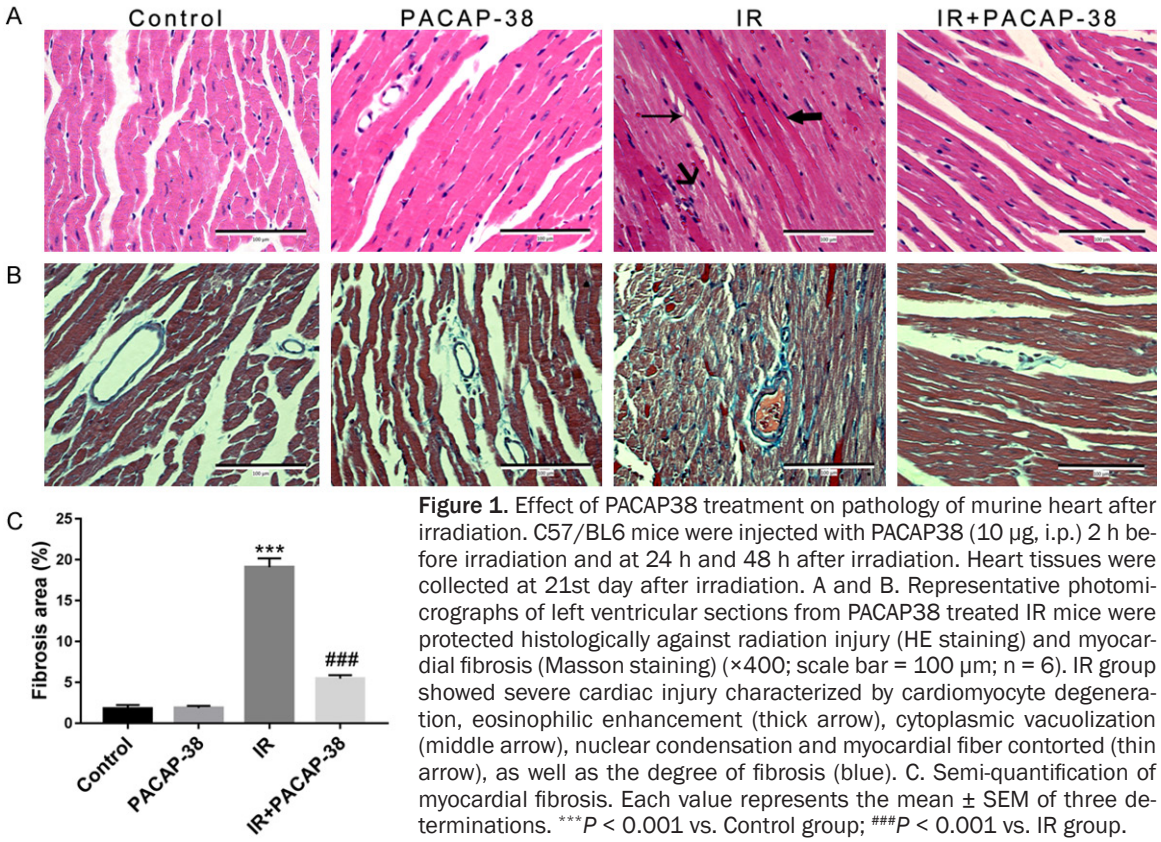

Figure 1. Effect of PACAP38 treatment on pathology of murine heart after irradiation. C57/BL6 mice were injected with PACAP38 (10 μg, i.p.) 2 h before irradiation and at 24 h and 48 h after irradiation. Heart tissues were collected at 21st day after irradiation. A and B. Representative photomicrographs of left ventricular sections from PACAP38 treated IR mice were protected histologically against radiation injury (HE staining) and myocardial fibrosis (Masson staining) (×400; scale bar = 100 μm; n = 6). IR group showed severe cardiac injury characterized by cardiomyocyte degeneration, eosinophilic enhancement (thick arrow), cytoplasmic vacuolization (middle arrow), nuclear condensation and myocardial fiber contorted (thin arrow), as well as the degree of fibrosis (blue). C. Semi-quantification of myocardial fibrosis. Each value represents the mean ± SEM of three determinations. $^{***}P < 0.001$ vs. Control group; $^{###}P < 0.001$ vs. IR group.

Effects of PACAP38 on myocardial cell toxicity and ROS generation after IR injury

We determined cytoxicity and cellular ROS level in the cultures of H9C2 cells treated with 10^{-7} M and 10^{-9} M PACAP38 2 h prior to 12 Gy X-ray IR. The cytotoxicity was determined at 48 h after IR by CCK8 assay. As shown in **Figure 3A**, cell viability was significantly decreased to 83.67 ± 0.78% (P < 0.001) after IR. Treatment with PACAP38 markedly suppressed the IR-induced myocardial cell toxicity dose-dependently (98.63 ± 2.70% and 92.57 ± 0.82% after 10^{-7} M and 10^{-9} M PACAP38 treatments, respectively, **Figure 3A**) and led to an increase on colony-forming efficiency at IR doses of 2 Gy, 4 Gy and 8 Gy (**Figure 3B**) in wild-type H9C2 cultures. Moreover, the SF2 (survival fraction at 2 Gy) was increased from 0.526 to 0.629 or 0.699, and the SER (survival enhancement ratio) was 0.953 or 0.905, by 10^{-9} M or 10^{-7} M PACAP38 treated H9C2 cells (**Figure 3C** and **Table 2**). The results suggested that PACAP38 reduced radiosensitivity of H9C2 cardiomyoblast cells.

We also performed DCFH-DA fluorescence assay to measure cellular ROS level following IR which apparently increased the ROS level in H9C2 cells ($P < 0.01$). Of interest, PACAP38 administration (10^{-7} M or 10^{-9} M) even after 48 h of IR resulted in significant suppression of intracellular ROS generation induced by radiation in a dose-dependent manner (**Figure 4A** and **4B**, $P < 0.01$ and $P < 0.05$), although the magnitude of ROS production and cell viability remain no obvious impact on H9C2 cells by PACAP38 treatment alone.

Antiapoptotic effect of PACAP38 on IR-induced myocardial cell injury

After demonstrating that PACAP38 has an inhibitory effect against IR-induced apoptosis in myocardium *in vivo*, we attempted to mimic IR in cell cultures by exposing myocardial cells to radiation. PACAP38 (10^{-7} M or 10^{-9} M) was added 2 h before subjecting cells to IR. The effect of PACAP38 on myocardial cell apoptosis was monitored by fluorescence-activated cell sorting analysis as described previously. The fraction of active fluorescein isothiocyanate (FITC)-labeled annexin V-positive (apoptotic) cells was increased significantly from 11.86 ± 2.77% to 65.07 ± 1.37% by IR, but was reduced

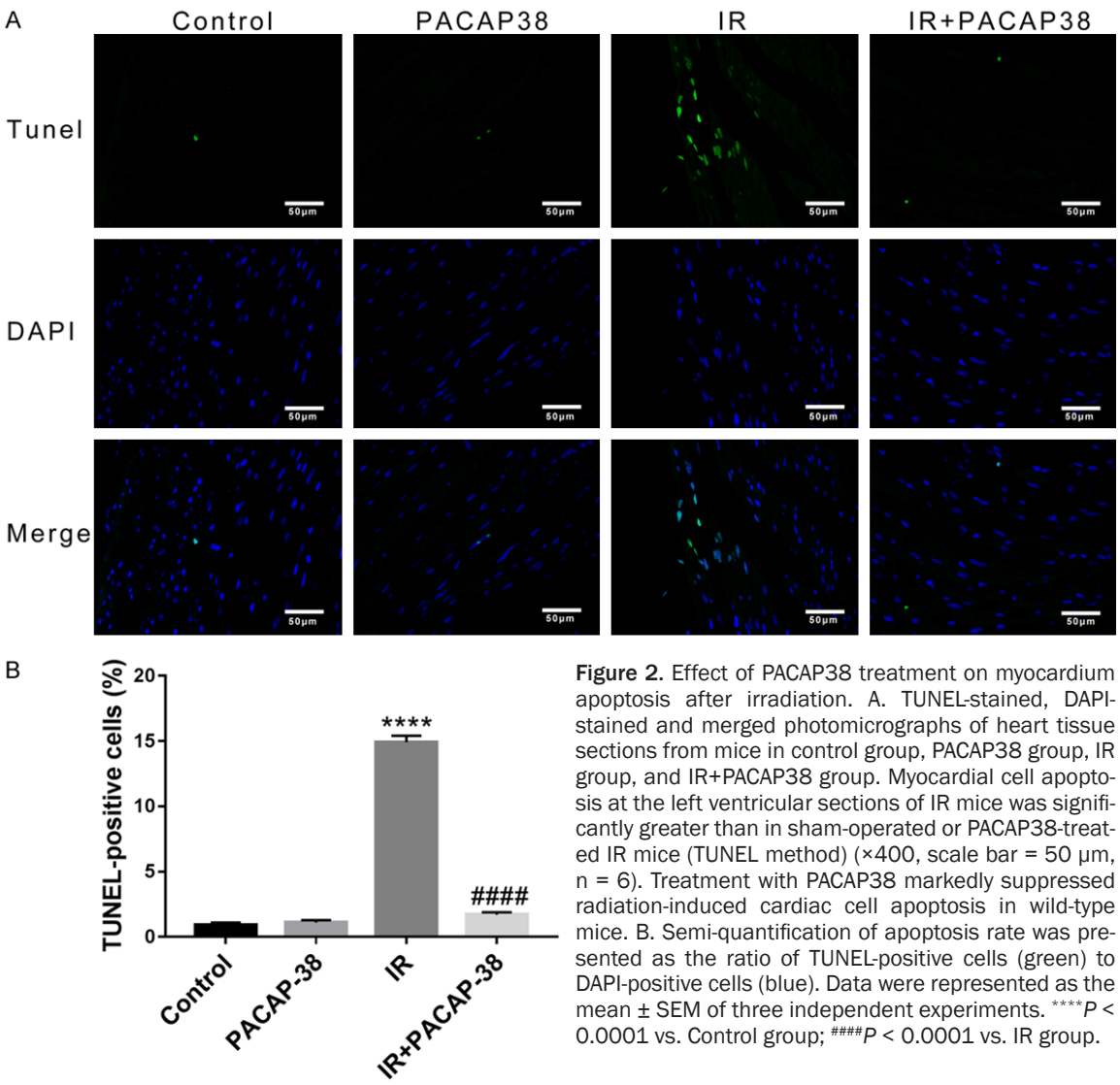

Figure 2. Effect of PACAP38 treatment on myocardium apoptosis after irradiation. A. TUNEL-stained, DAPI-stained and merged photomicrographs of heart tissue sections from mice in control group, PACAP38 group, IR group, and IR+PACAP38 group. Myocardial cell apoptosis at the left ventricular sections of IR mice was significantly greater than in sham-operated or PACAP38-treated IR mice (TUNEL method) (×400, scale bar = 50 μm, n = 6). Treatment with PACAP38 markedly suppressed radiation-induced cardiac cell apoptosis in wild-type mice. B. Semi-quantification of apoptosis rate was presented as the ratio of TUNEL-positive cells (green) to DAPI-positive cells (blue). Data were represented as the mean ± SEM of three independent experiments. $^{****}P < 0.0001$ vs. Control group; $^{####}P < 0.0001$ vs. IR group.

sharply from 65.07 ± 1.37% to 40.28 ± 3.29% ($P < 0.001$) or 52.83 ± 1.61% ($P < 0.05$) by PACAP38 treatment (10^{-7} M or 10^{-9} M, respectively) (**Figure 5A**, **5B**) in wild-type cells. In contrast, PACAP38 treatment alone had no obvious effect on the apoptotic rate.

The apoptosis-related mRNA and protein expressions of Bcl2 and Bax were determined by qRT-PCR and Western blot to elucidate the molecular mechanism of PACAP38 alleviating IR-induced apoptosis. **Figure 5C-G** shows the expressions of both mRNA (**Figure 5C**, **5D**) and protein (**Figure 5E-G**) of the proapoptotic gene Bax were notably elevated, whereas the anti-apoptotic gene Bcl2 were markedly decreased in wild-type myocardial cells exposed to IR. Yet, with 10^{-7} M or 10^{-9} M PACAP38 pre-treatment, the elevation of Bax level was inhibited and the suppression of Bcl2 level was also rescued following cardiac IR (**Figure 5C-G**) in H9C2 cardiomyoblast cells at the basal level, revealing a cytoprotective effect of PACAP38 on myocardial cell apoptosis partially dependent of pro-apoptotic gene-regulated signaling.

Effects of PACAP38 on IR-induced G2/M arrest and cell cycle-associated protein expression in myocardial cells

The effect of PACAP38 on IR-induced cell cycle distribution was analyzed by flow cytometry (**Figure 6A**, **6B**). The fraction of cells at G2/M phase was markedly increased in the IR group (9.84 ± 0.30% control vs. 20.60 ± 0.06% IR, $P < 0.0001$). In contrast, in PACAP38 (10^{-7} M)

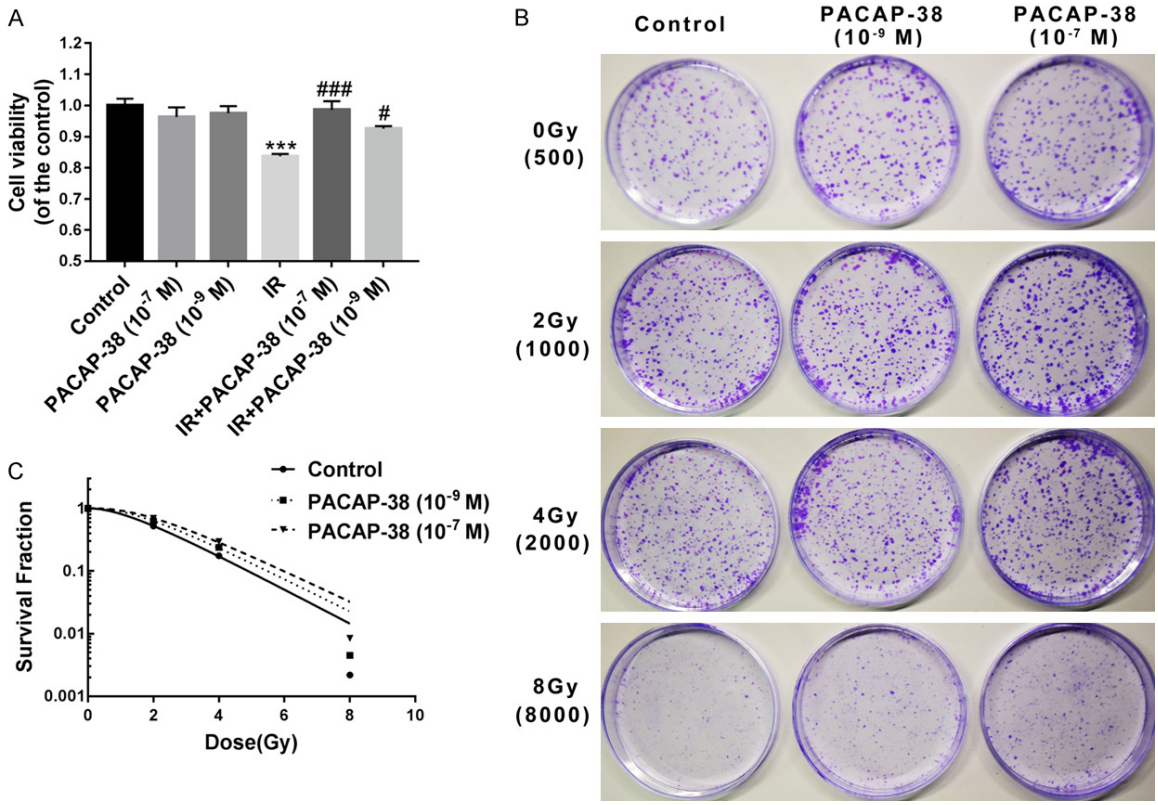

Figure 3. The protective role of PACAP38 against IR-induced cytotoxicity in H9C2 cells. A. H9C2 cells were pretreated with PACAP38 (10^{-9} or 10^{-7} M) 2 h before 12 Gy X-rays irradiation. Cell viability was determined by CCK8 assay at 48 h after IR. B. PACAP38 decreased the radiosensitivity of H9C2 cells at a variety of IR doses (0, 2, 4, 8 Gy) using clone formation assay. The implanted cells were increased with IR doses (500-8000 cells/dish). C. The survival fraction data were fitted into the single-hit multitarget model. The formula: $SF=1-(1-e^{-D/D0})^n$. Survival curves were drawn by Graphpad Prism. The results were expressed as the means ± SEM of three independent experiments. $^{***}P < 0.001$ vs. Control group; $^{###}P < 0.001$, $^{#}P < 0.05$ vs. IR group.

Table 2. The effect of PACAP38 on the radiosensitivity of H9C2 cells

	D0	Dq	SF2	SER
Control	1.589 ± 0.010	1.275 ± 0.066	0.526 ± 0.016	1
PACAP38 (10^{-9} M)	1.668 ± 0.033*	1.700 ± 0.055*	0.629 ± 0.009**	0.953 ± 0.021*
PACAP38 (10^{-7} M)	1.760 ± 0.063**	1.990 ± 0.111**	0.699 ± 0.020**	0.905 ± 0.034**

Data were fit into the single-hit multi-target model. Data were expressed as the mean ± SEM. $^{*}P < 0.05$ and $^{**}P < 0.01$ vs. the corresponding untreated control group. D0, the mean lethal dose; Dq, quasi-threshold dose; SF2, survival fraction at irradiation dose of 2 Gy; SER, survival enhancement ratio.

treated-IR group, the G2/M cell fraction was modestly decreased from 20.60 ± 0.06% to 15.41 ± 0.11% ($P < 0.0001$), revealing that PACAP38 reversed IR-induced G2/M arrest of myocardial cells. But 10^{-9} M PACAP38 was not seen effect.

The expressions of CDC2 and cyclinB1 regulated G2/M control point of cell cycle were also examined by qRT-PCR and Western blot analyses. Consistant to the upper results, both transcript (**Figure 6C**, **6D**) and protein (**Figure 6E-G**) levels of CDC2 and cyclinB1 were significantly reduced at 48 h after 12 Gy X-ray irradiation as comparing with the control group ($P < 0.01$). However, pre-treatment with 10^{-7} M PACAP38 significantly reversed the expressions of CDC2 and cyclinB1 ($P < 0.05$).

PACAP38 promoted IR-induced NRF2/HO-1 signaling activation in myocardial cells

NRF2 activation leads to nuclear translocation and promotes transcription of HO-1 signaling

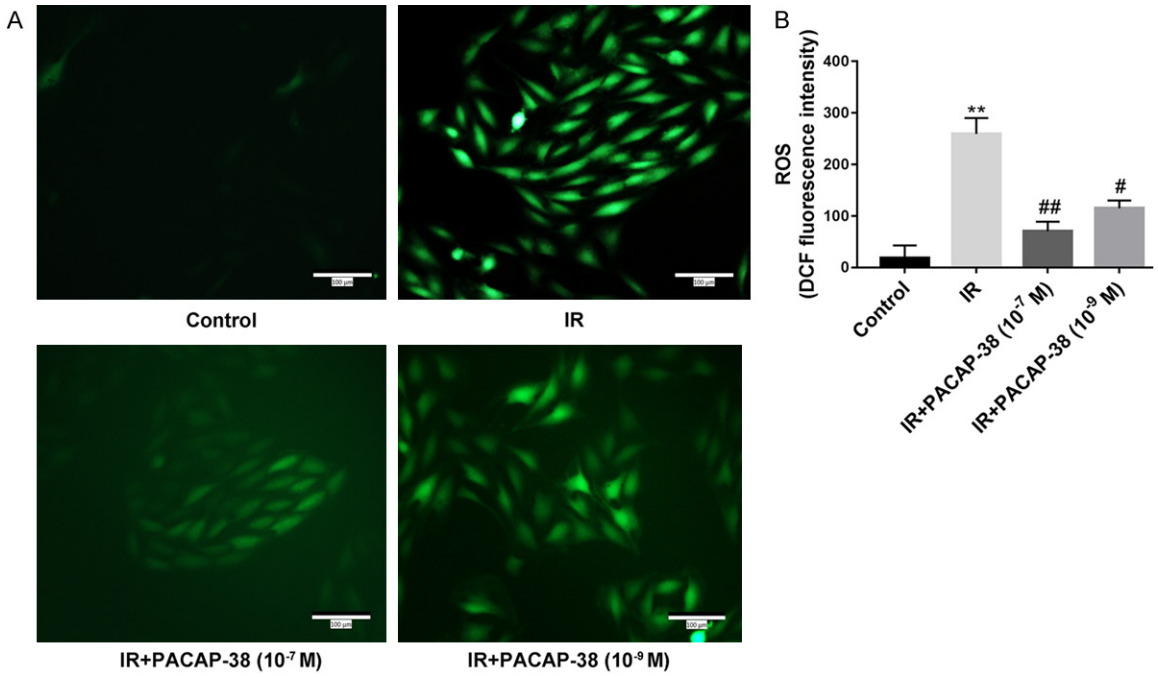

Figure 4. Effects of PACAP38 treatment on ROS level in H9C2 cells after radiation injury. A. H9C2 cells were pre-treated with PACAP38 (10^{-9} or 10^{-7} M) 2 h before 12 Gy X-rays irradiation. 48 h after IR, H9C2 cells stained with DCFH-DA were observed with fluorescence microscopy (×200; scale bar = 100 μm). B. Semi-quantitative analysis of ROS production. Each value represents the mean ± SEM of three independent experiments. $^{**}P < 0.01$ vs. Control group; $^{\#}P < 0.05$, $^{\#\#}P < 0.01$ vs. IR group.

pathway. NRF2 and HO-1 are key factors of anti-oxidative stress in cardiomyocytes [21]. To determine the role of NRF2/HO-1 activation and whether PACAP38 can enhance NRF2/HO-1 to prevent myocardial cells injury after IR, we pretreated myocardial cells with PACAP38 prior to radiation injury. The presence of the mRNA for NRF2 and HO-1 was verified in cultures of H9C2 cardiomyoblast cells by qRT-PCR (**Figure 7A**, **7B**). The transcript expressions of NRF2 and HO-1 were increased moderately by IR ($P < 0.05$ compared to control) and further enhanced by PACAP38 (10^{-7} M or 10^{-9} M) + IR group ($P < 0.001$ or $P < 0.05$, respectively). In accordance with the mRNA expression changes, pre-treatment with 10^{-7} M PACAP38 further enhanced the protein expressions of NRF2 and HO-1 (**Figure 7C-E**).

Furthermore, NRF2-siRNA transfection was used to inhibit the expression of NRF2 and its target gene HO-1. Treatment of cells with NRF2-siRNA-2 efficiently knocked down the transcript expressions of NRF2 and HO-1 (**Figure 8A**, $P < 0.01$), as well as the protein expressions (**Figure 8B** and **8C**, $P < 0.0001$). Analysis of mRNA extracted from cells revealed that this was a consequence of decreased transcription. Knockdown of NRF2 by siRNA eliminated the PACAP38 enhanced NRF2 and HO-1 upregulation in the absence or presence of radiation exposure (**Figure 8D-H**, $P < 0.05$). As shown in **Figure 8I**, cell viability was significantly reduced in IR group (IR vs. NC, $P < 0.001$) and was almost completely recovered with 10^{-7} M PACAP38 administration (PACAP38+IR vs. IR, $P < 0.01$). NRF2 interference had no effect on cell viability but increased cell sensitivity to IR (SiNRF2+IR vs. IR, $P < 0.05$). Moreover, NRF2-siRNA transfection partially eliminated the protective effect of PACAP38 against IR-induced cell death (PACAP38+SiNRF2+IR vs. PACAP38+IR, $P < 0.05$) in myocardial cells.

Discussion

RIHD is associated with prolonged follow up and to certain degree, offsets the long-term survival benefits of radiotherapy for thoracic malignant tumors. The process of oxidative stress and proinflammatory response is associated with the development of RIHD. A meta-analysis of Early Breast Cancer Trialists' Collaborative Group (EBCTCG) indicated that a sig-

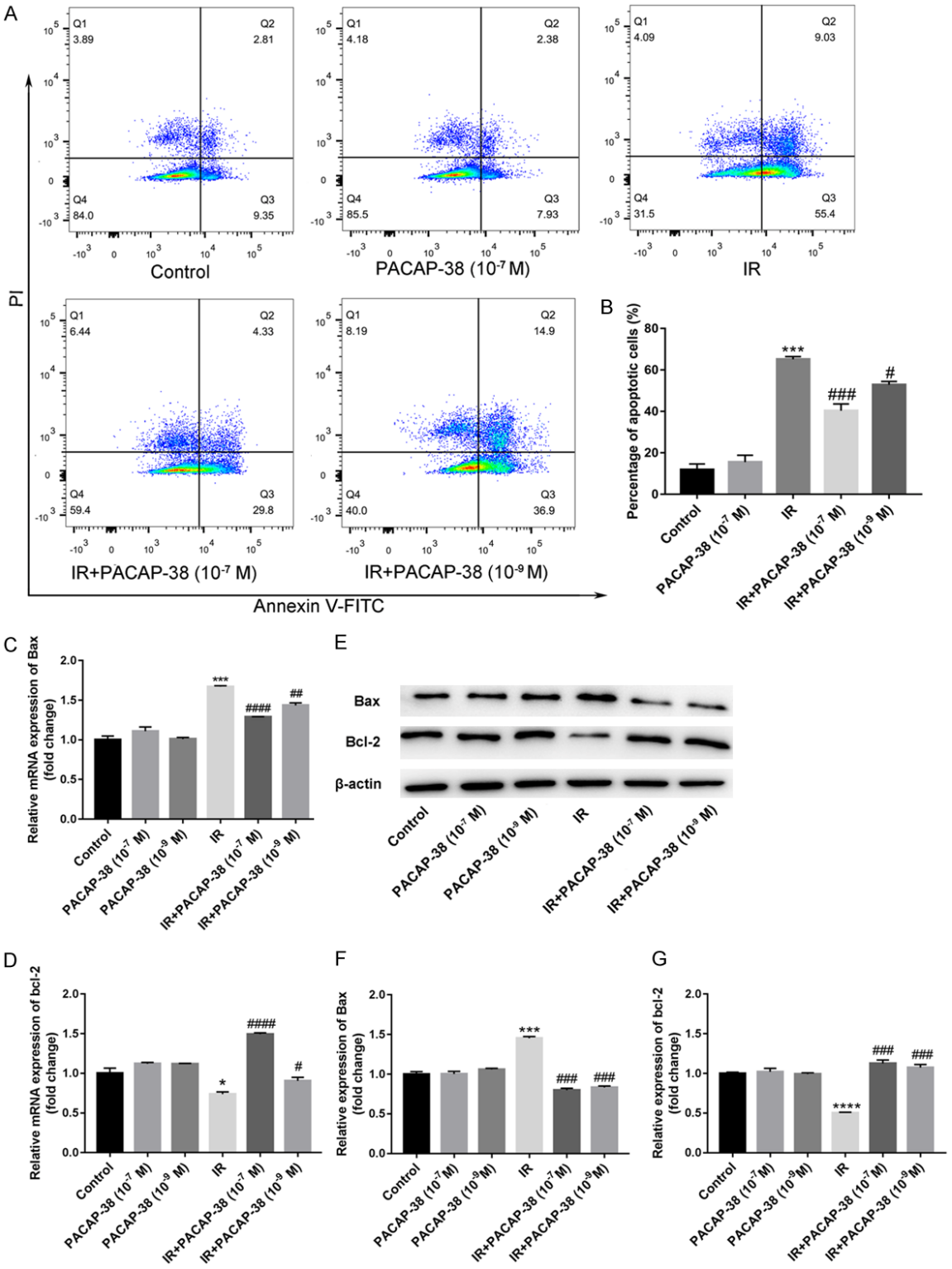

Figure 5. Antiapoptotic effects of PACAP38 on the apoptotic rates and the expressions of Bax and Bcl-2 in H9C2 cells after radiation exposure. PACAP38 (10^{-9} or 10^{-7} M) was added 2 h before 12 Gy X-rays irradiation in H9C2 cell cultures. Apoptosis was examined at 48 h by fluorescence-activated cell sorting analysis (A). The fraction of active FITC-annexin V-positive cells was increased significantly from 11.86% to 65.07% by irradiation and was reduced sharply from 65.07% to 40.28% or 52.83% by 10^{-7} M or 10^{-9} M PACAP38 treatment in wild-type cells (B). (C, D) PACAP38 (10^{-9} or 10^{-7} M) reversed IR-induced the proapoptotic gene Bax and Bcl-2 mRNA levels by qRT-PCR. (E-G)

Western blot analysis of Bax and Bcl-2 protein expressions. The results were expressed as the mean ± SEM of 3 independent experiments. $^{*}P < 0.05$, $^{***}P < 0.001$, $^{****}P < 0.0001$ vs. Control group; $^{\#}P < 0.05$, $^{\#\#}P < 0.01$, $^{\#\#\#}P < 0.001$, $^{\#\#\#\#}P < 0.0001$ vs. IR group.

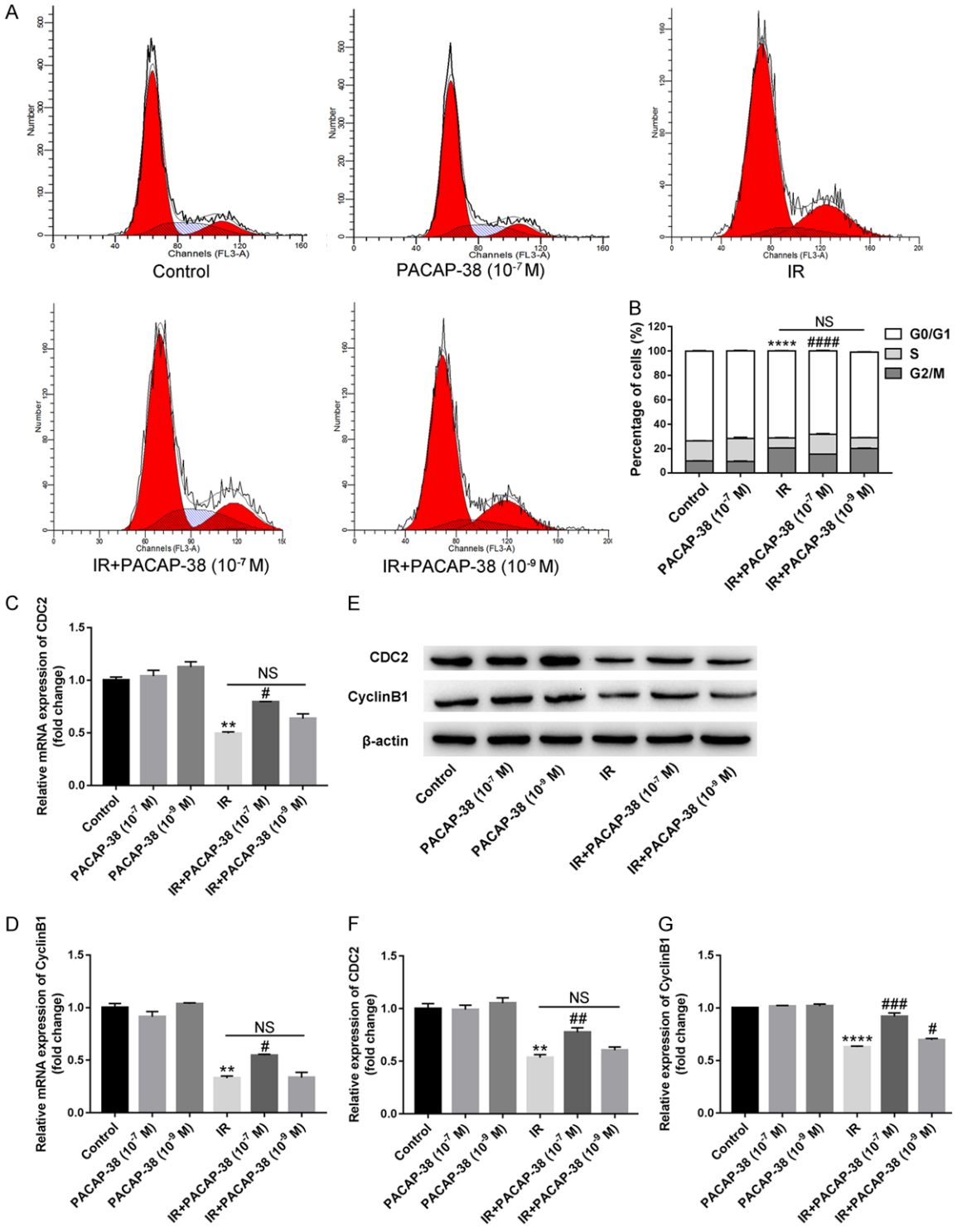

Figure 6. Effects of PACAP38 treatment on the cell cycle distribution and related expressions of CDC2 and CyclinB1 in radiation exposed H9C2 cells. H9C2 cells were pre-treated with PACAP38 (10^{-9} or 10^{-7} M) for 2 h before radiation exposure and cultured for 48 h. A. PACAP38 recovered IR-induced G2/M arrest at a concentration of 10^{-7} M. The cell cycle distribution was determined by flow cytometry with PI staining. B. Quantitative analysis of cell cycle distribu-

tion. C, D. PACAP38 (10^{-7} M) reversed the down-regulation of CDC2 and CyclinB1 mRNA expression induced by IR. E-G. The protein expressions of CDC2 and CyclinB1 were evaluated by Western blot. The results were expressed as the mean ± SEM of 3 independent experiments. $^{**}P < 0.01$, $^{****}P < 0.0001$ vs. Control group; $^{\#}P < 0.05$, $^{\#\#}P < 0.01$, $^{\#\#\#}P < 0.001$, $^{\#\#\#\#}P < 0.0001$ vs. IR group. NS indicates no significance.

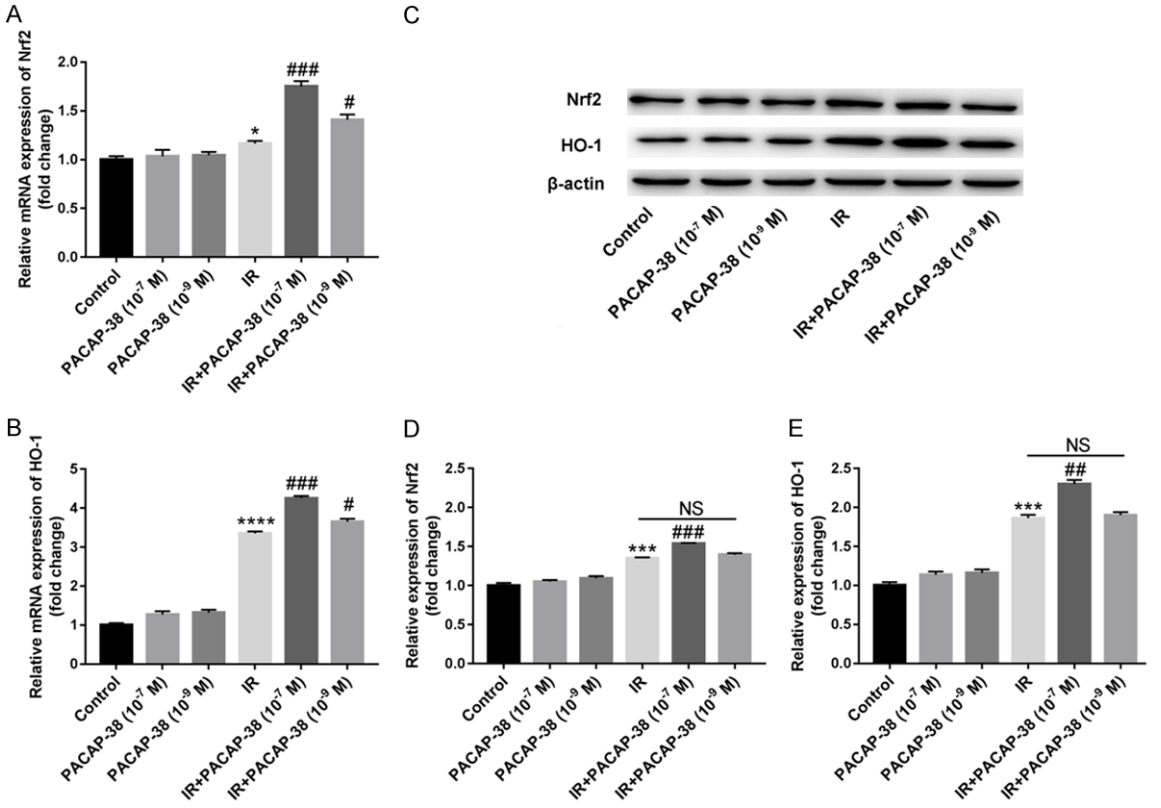

Figure 7. Effects of PACAP38 treatment on the expression of Nrf2/HO-1 signaling in H9C2 cells exposed to radiation. H9C2 cells were administrated with PACAP38 (10^{-9} or 10^{-7} M) for 2 h before X-rays irradiation and were post-cultured for 48 h. A, B. PACAP38 (10^{-9} or 10^{-7} M) further enhanced the up-regulation of Nrf2 and HO-1 mRNA expression induced by IR. C-E. The protein expressions of Nrf2 and HO-1 were analyzed by immunoblots. Exposure to radiation led to increase of Nrf2 and HO-1 expression, and 10^{-7} M PACAP38 treatment promoted these responses substantially *in vitro*. Each value was represented as the mean ± SEM of 3-4 determinations in 3 replicate experiments. $^{*}P < 0.05$, $^{***}P < 0.001$, $^{****}P < 0.0001$ vs. the corresponding untreated control group; $^{\#}P < 0.05$, $^{\#\#}P < 0.01$, $^{\#\#\#}P < 0.001$ vs. the samples subjected to IR, respectively. NS = no significance.

nificant excess of heart diseases mortality (RR = 1.27) in patients treated with radiation [5]. Modern techniques have significantly decreased both dose and volume to the heart. Nevertheless, radiation dose will not be zero despite all the technical progress. Thus, it is important to explore new protective strategy against RIHD. Several attempts have been made in clinical treatment of RIHDs: Amifostine, a radioprotector approved by FDA in 1995 [22], has failed to use in routine radiotherapy currently because of its side effects (vomiting, nausea, and hypotension) [23]. Moreover, angiotensin converting enzyme inhibition has also been reported as a promising therapeutic strategy to reduce cardiopulmonary complications induced by radiotherapy [24]. However, its application perspective was offset by the side effects involving angioedema, hypotension and debilitating cough caused by bradykinin accumulation. There is an increasing need for an effective and nontoxic phamacological agent in order to prevent and treat RIHDs.

As an endogenous peptide, PACAP is a naturally occurring pleiotropic peptide that plays an important role in the early responses to tissue injury subsequent to ischemia and hypoxia [25]. PACAP38 has been defined potent cytoprotective roles based on its anti-inflammatory,

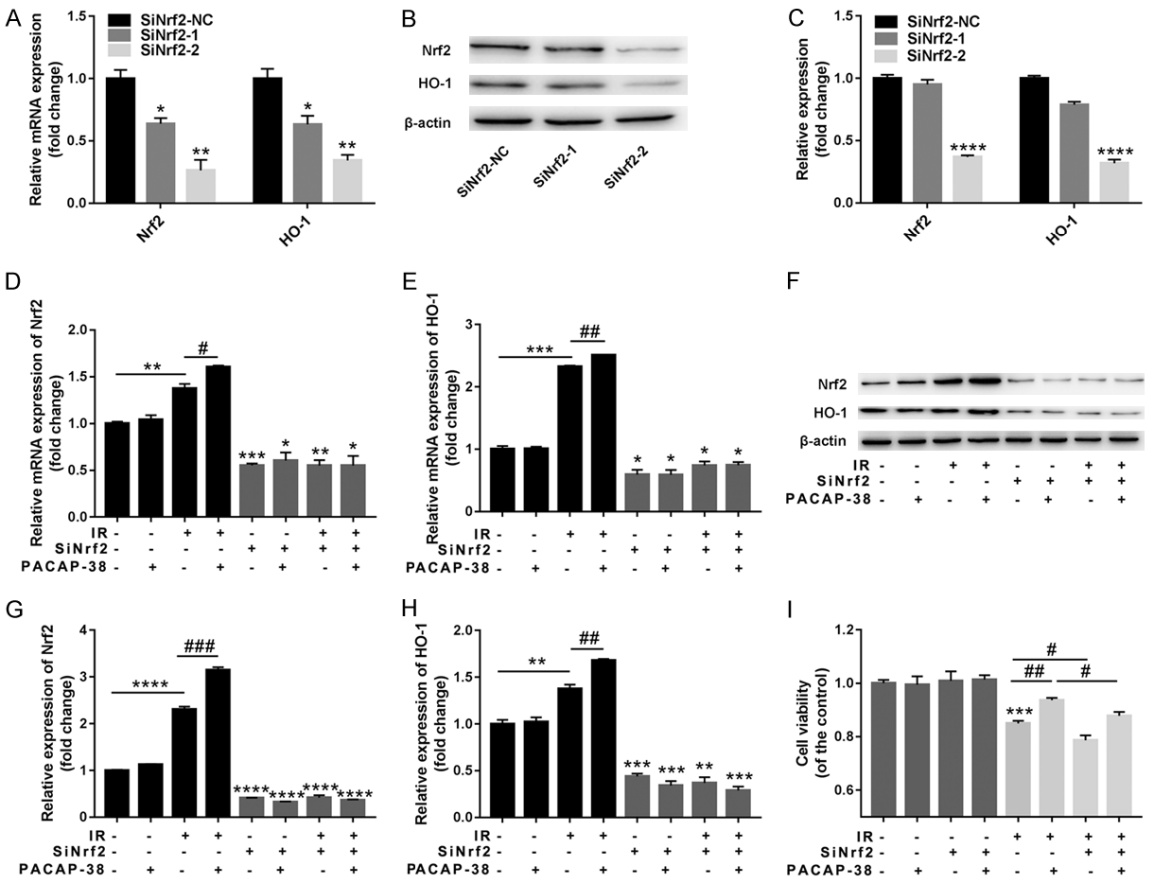

Figure 8. Effects of Nrf2-siRNA transfection on the activation of Nrf2 signaling and cytoprotection of PACAP38 in H9C2 cells exposed to radiation. (A-C) H9C2 cells were transiently transfected with two different Nrf2-specific siRNA (SiNrf2-1 and SiNrf2-2). The mRNA (A) and protein (B and C) expressions of Nrf2 and HO-1 were determined by qRT-PCR and Western blotting at 48 h after transfection. SiNrf2-2 efficiently knocked down Nrf2 expressions. $^{**}P < 0.01$ vs. SiNrf2-NC. (D-I) After 24 h of SiNrf2 transfection, H9C2 cells were treated with 10^{-7} M PACAP38 for 2 h before IR. The transcripts (D, E) and protein (F-H) expressions of Nrf2 and HO-1 were examined by qRT-PCR and Western blot analyses at 48 h after IR. Cell viability was measured by CCK8 assay (I). Pretreatment with SiNrf2 almost completely abolished the increases in Nrf2 and HO-1 expressions enhanced by PACAP38 in culture of H9C2 cells following radiation. The cell viability did not completely reduced by knockdown of SiNrf2 in the presence of PACAP38 and IR treatments, suggesting the existence of Nrf2-independent cardioprotective pathway activated by PACAP38. Each value was represented as the mean ± SEM of 3-4 determinations in 3 replicate experiments. $^{*}P < 0.05$, $^{**}P < 0.01$, $^{***}P < 0.001$, $^{****}P < 0.0001$ vs. the corresponding untreated control group; $^{\#}P < 0.05$, $^{\#\#}P < 0.01$, $^{\#\#\#}P < 0.001$ vs. the samples subjected to IR, respectively, or according to the label (-).

anti-apoptotic and antioxidant activities. In the heart, PACAP38 has positive chronotropic and inotropic effects, as well as the ability to dilate blood vessels [26-28]. In our study, using rat cardiomyocytes and murine heart exposed to radiation, we found that PACAP38 significantly activated the expression of NRF2/HO-1, a key factor of anti-oxidative stress in cardiomyocytes, and reduced the apoptosis, oxidative reaction, cardiomyocyte degeneration, and cell cycle arrest of myocardial cells with irradiation. PACAP38 could effectively recover tissue damage as well as cardiac fibrosis of mouse heart by irradiation *in vivo*. The cardioprotective function of PACAP38 was partially blocked by transient knockdown of NRF2, highlighting the pivotal role of NRF2/HO-1 signaling in cardioprotective effect of PACAP38 on cardiac radiation toxicity. The results encourage the attempt to develop effective tool for *de novo* intervention of myocardial injury subsequent to radiation treatment of thoracic neoplasms.

In RIHD, cellular and tissue injuries occur early during oxidative reaction phase, exerted by producing reactive oxygen species (ROS) to induce

oxidative damage to cellular structures [29]. Our findings showed that IR markedly increased the intracellular ROS level of H9C2 cells. PACAP38 treatment significantly suppressed the production of ROS to a greater extent in cardiomyocytes. Substantial evidence demonstrates that acute overload of ROS displays important sensitizing effect on pathogenesis of cardiovascular disease [30]. The overproduction of ROS could promote the activation of NRF2, a major endogenous antioxidant molecule, further to increase the subsequent expression of HO-1 and other antioxidant related molecules in response to IR-induced cardiac injury. Activation of the NRF2 signaling plays central role that reduces cell damage caused by radiation-induced oxidative stress [31, 32]. Interestingly, our experiments in vitro in cardiomyocyte cultures demonstrated that irradiation could result in compensatory activation of NRF2 and HO-1 expressions which were further promoted by the administration of PACAP38. Furthermore, cytotoxinic effect of ionizing radiation was aggravated by NRF2 interference, which also partially blocked the protective effect of PACAP38. As it is known that HO-1 has a downstream signaling pathway dependent of NRF2, genetic knockdown of NRF2 significantly reduced the expression of HO-1 and appeared increased vulnerability to IR injury in heart beyond the regulation of proinflammatory response, providing novel evidence that HO-1 also participates in enhancement of PACAP modulated cytoprotective effect. Our results demonstrated that activation of NRF2/HO-1 is critical for cardioprotective action of PACAP38 in myocardial cells in response to irradiation. The protective effect of PACAP38 on myocardium responses to radiation injury may involve both NRF2-dependent and -independent pathways, which remains to be studied.

On the other hand, the levels of apoptosis are highly correlated with the severity of the pathological response to radiation-induced cardiac injury [33]. PACAP38 has been reported to inhibit apoptosis in cardiomyopathy through triggering the transduction signals to promote the expression of Bcl-2 which blocks the release of cytochrome c and inhibits the activation of caspase [18]. PACAP also inhibits the expression of proapoptotic factors such as c-Jun or Bax [19]. Our results demonstrated that radiation-induced cardiomyocytes apoptosis was effectively reduced by pre-treatment of PACAP-38 through regulating the expression of apoptosis-related proteins Bax and Bcl2. Moreover, we also found that PACAP38 reversed radiation-induced cardiomyocytes G2/M arrest by regulating the expression of CDC2 and cyclinB1 in H9C2 cells. Downregulation of the expression of CDC2 and CyclinB1 induces G2/M cell cycle arrest. Our results suggested that the protective effects of PACAP38 may also involve reversing G2/M cell cycle arrest.

Moreover, the IR-induced myocardial fibrosis including perivascular fibrosis after irradiation at 21 days was suppressed by PACAP38 treatment as shown by histological evaluation. Perivascular fibrosis is considered as a leading pathway to myocardial ischemia and RIHD [34]. Furthermore, pretreatment with PACAP38 even after early stage of myocardial damage was still protective and effectively controlled perivascular fibrosis in vivo in animal model of RIHD. Additional in vivo studies in mice with the administration of PACAP38 after the cycle of ischemia would greatly enhance development of a clinical treatment. In addition, a variety of cardiac substructures, including coronary artery, pericardium, myocardium, valves, and conduction system are involved in the occurrence sites of RIHDs. In our study, the protective effects of PACAP38 were evaluated mainly on myocardium which accounts for the largest proportion of the heart. The effects of PACAP38 on cardiac substructures and the molecular mechanism against RIHD remain further investigation.

In summary, our findings indicated the protective effects of PACAP38 on acute radiation-induced myocardial injury in vitro and in vivo, manifested by inhibiting apoptosis, cell cycle arrest, oxidative reaction, fibrosis, and further promoting Nrf2/HO-1-dependent signaling activation which is essential for the RIHD. The enhancement and promoting NRF2/HO-1-dependent signaling is required to a large extent for the cardioprotective effects of PACAP38 on IR-induced myocardial toxicity, although there is possible for a relatively small further cytoprotective effect independent of NRF2/HO-1. The efficacy of PACAP38 as a cardioprotectant in mice exposed to radiation could provide the rationale for using PACAP38 as a simple nontoxic protective agent and an effective therapy for RIHD. However, gap exists regarding translating these results into clinical therapeutic

strategy. Further translational studies are largely required to further evaluate its pharmacodynamics and therapeutic efficacy. Encouragingly, our findings were the first direct evidence of therapeutic potential of PACAP38 on radiation-induced cardiac injury.

Acknowledgements

This work was supported in part by the National Natural Science Foundation of China (grants 81673102, 81602791, 81803164 and 81972963) and National Key Research and Development Program of China (grant 2016YFC0105409); Shanghai Municipal Education Commission-Gaofeng Clinical Medicine Grant Support (grant 20171904); Youth Foundation of Shanghai Health and Family Planning Commission (grant 20164Y0066) and Special construction of integrated Chinese and Western medicine in general hospital (grant ZHYY-ZXYJHZ X-2-201704). The authors declare no conflicts of interest.

Disclosure of conflict of interest

None.

Address correspondence to: Jia-Yi Chen and Min Li, Department of Radiation Oncology, Ruijin Hospital, Shanghai Jiaotong University School of Medicine, 197 Ruijin Er Road, Shanghai 200025, China. Tel: +86-21-64370045; Fax: +86-21-6415688; E-mail: chenjiayi0188@aliyun.com (JYC); lm11866@rjh.com.cn (ML)

References

[1] Delaney G, Jacob S, Featherstone C and Barton M. The role of radiotherapy in cancer treatment: estimating optimal utilization from a review of evidence-based clinical guidelines. Cancer 2005; 104: 1129-1137.

[2] Van Nimwegen FA, Ntentas G, Darby SC, Schaapveld M, Hauptmann M, Lugtenburg PJ, Janus CPM, Daniels L, van Leeuwen FE, Cutter DJ and Aleman BMP. Risk of heart failure in survivors of Hodgkin lymphoma: effects of cardiac exposure to radiation and anthracyclines. Blood 2017; 129: 2257-2265.

[3] Van Nimwegen FA, Schaapveld M, Janus CP, Krol AD, Petersen EJ, Raemaekers JM, Kok WE, Aleman BM and van Leeuwen FE. Cardiovascular disease after hodgkin lymphoma treatment. JAMA Intern Med 2015; 175: 1007-17.

[4] Adams MJ, Lipsitz SR, Colan SD, Tarbell NJ, Treves ST, Diller L, Greenbaum N, Mauch P and Lipshultz SE. Cardiovascular status in long-term survivors of Hodgkin's disease treated with chest radiotherapy. J Clin Oncol 2004; 22: 3139-48.

[5] Clarke M, Collins R, Darby S, Davies C, Elphinstone P, Evans V, Godwin J, Gray R, Hicks C, James S, Mackinnon E, McGale P, McHugh T, Peto R, Taylor C and Wang Y. Effects of radiotherapy and of differences in the extent of surgery for early breast cancer on local recurrence and 15-year survival: an overview of the randomised trials. Lancet 2005; 66: 2087-2106.

[6] McGale P, Darby SC, Hall P, Adolfsson J, Bengtsson NO, Bennet AM, Fornander T, Gigante B, Jensen MB, Peto R, Rahimi K, Taylor CW and Ewertz M. Incidence of heart disease in 35,000 women treated with radiotherapy for breast cancer in Denmark and Sweden. Radiother Oncol 2011; 100: 167-75.

[7] Hooning MJ, Aleman BM, van Rosmalen AJ, Kuenen MA, Klijn JG and van Leeuwen FE. Cause-specific mortality in long-term survivors of breast cancer: a 25-year follow-up study. Int J Radiat Oncol Biol Phys 2006; 64: 1081-91.

[8] Zhu Q, Kirova YM, Cao L, Arsene-Henry A and Chen J. Cardiotoxicity associated with radiotherapy in breast cancer: a question-based review with current literatures. Cancer Treat Rev 2018; 68: 9-15.

[9] Darby SC, Cutter DJ, Boerma M, Constine LS, Fajardo LF, Kodama K, Mabuchi K, Marks LB, Mettler FA, Pierce LJ, Trott KR, Yeh ET and Shore RE. Radiation-related heart disease: current knowledge and future prospects. Int J Radiat Oncol Biol Phys 2010; 76: 656-665.

[10] Citrin DE and Mitchell JB. Mechanisms of normal tissue injury from irradiation. Semin Radiat Oncol 2017; 27: 316-24.

[11] Wallace SS. Enzymatic processing of radiation-induced free radical damage in DNA. Radiat Res 1998; 150: S60-S79.

[12] Loboda A, Damulewicz M, Pyza E, Jozkowicz A and Dulak J. Role of Nrf2/HO-1 system in development, oxidative stress response and diseases: an evolutionarily conserved mechanism. Cell Mol Life Sci 2016; 73: 3221-47.

[13] Cominacini L, Mozzini C, Garbin U, Pasini A, Stranieri C, Solani E, Vallerio P, Tinelli IA and Fratta Pasini A. Endoplasmic reticulum stress and Nrf2 signaling in cardiovascular diseases. Free Radic Biol Med 2015; 88: 233-242.

[14] Li Q, Xiang Y, Chen Y, Tang Y and Zhang Y. Ginsenoside Rg1 protects cardiomyocytes against hypoxia/reoxygenation injury via activation of Nrf2/HO-1 signaling and inhibition of JNK. Cell Physiol Biochem 2017; 44: 21-37.

[15] Sherwood NM, Krueckl SL and McRory JE. The origin and function of the pituitary adenylate cyclase-activating polypeptide (PACAP)/gluca-

gon superfamily. Endocr Rev 2000; 21: 619-670.
[16] Vaudry D, Falluel-Morel A, Bourgault S, Basille M, Burel D, Wurtz O, Fournier A, Chow BK, Hashimoto H, Galas L and Vaudry H. Pituitary adenylate cyclase-activating polypeptide and its receptors: 20 years after the discovery. Pharmacol Rev 2009; 61: 283-357.
[17] Gasz B, Rácz B, Röth E, Borsiczky B, Tamás A, Boronkai A, Gallyas FJ, Tóth G and Reglodi D. PACAP inhibits oxidative stress-induced activation of MAP kinase-dependent apoptotic pathway in cultured cardiomyocytes. Ann N Y Acad Sci 2006; 1070: 293-297.
[18] Racz B, Reglodi D, Horvath G, Szigeti A, Balatonyi B, Roth E, Weber G, Alotti N, Toth G and Gasz B. Protective effect of PACAP against doxorubicin-induced cell death in cardiomyocyte culture. J Mol Neurosci 2010; 42: 419-427.
[19] Seaborn T, Masmoudi-Kouli O, Fournier A, Vaudry H and Vaudry D. Protective effects of pituitary adenylate cyclase-activating polypeptide (PACAP) against apoptosis. Curr Pharm Des 2011; 17: 204-214.
[20] Mori H, Nakamachi T, Ohtaki H, Yofu S, Sato A, Endo K, Iso Y, Suzuki H, Takeyama Y, Shintani N, Hashimoto H, Baba A and Shioda S. Cardioprotective effect of endogenous pituitary adenylate cyclase-activating polypeptide on doxorubicin-induced cardiomyopathy in mice. Circ J 2010; 74: 1183-1190.
[21] Ndisang JF. Synergistic interaction between Heme Oxygenase (HO) and Nuclear-Factor E2-Related Factor-2 (Nrf2) against oxidative stress in cardiovascular related diseases. Curr Pharm Des 2017; 23: 1465-1470.
[22] Kouvaris JR, Kouloulias VE and Vlahos LJ. Amifostine: the first selective-target and broad-spectrum radioprotector. Oncologist 2007; 12: 738-747.
[23] Demiral AN, Yerebakan O, Simsir V and Alpsoy E. Amifostine-induced toxic epidermal necrolysis during radiotherapy: a case report. Jpn J Clin Oncol 2002; 32: 477-479.
[24] van der Veen SJ, Ghobadi G, de Boer RA, Faber H, Cannon MV, Nagle PW, Brandenburg S, Langendijk JA, van Luijk P and Coppes RP. ACE inhibition attenuates radiation-induced cardiopulmonary damage. Radiother Oncol 2015; 114: 96-103.
[25] Reglodi D, Vaczy A, Rubio-Beltran E and MaassenVanDenBrink A. Protective effects of PACAP in ischemia. J Headache Pain 2018; 19: 19.
[26] Farnham MM, Inglott MA and Pilowsky PM. Intrathecal PACAP-38 causes increases in sympathetic nerve activity and heart rate but not blood pressure in the spontaneously hypertensive rat. Am J Physiol Heart Circ Physiol 2011; 300: H214-22.
[27] Merriam LA, Roman CW, Baran CN, Girard BM, May V and Parsons RL. Pretreatment with non-selective cationic channel inhibitors blunts the PACAP-induced increase in guinea pig cardiac neuron excitability. J Mol Neurosci 2012; 48: 721-729.
[28] Clason TA, Girard BM, May V and Parsons RL. Activation of MEK/ERK signaling by PACAP in guinea pig cardiac neurons. J Mol Neurosci 2016; 59: 309-316.
[29] Taunk NK, Haffty BG, Kostis JB and Goyal S. Radiation-induced heart disease: pathologic abnormalities and putative mechanisms. Front Oncol 2015; 5: 39.
[30] Griendling KK and Fitzgerald GA. Oxidative stress and cardiovascular injury: part ii: animal and human studies. Circulation 2003; 108: 2034-2040.
[31] Yu J, Zhu X, Qi X, Che J and Cao B. Paeoniflorin protects human EA.hy926 endothelial cells against gamma-radiation induced oxidative injury by activating the NF-E2-related factor 2/heme oxygenase-1 pathway. Toxicol Lett 2013; 218: 224-34.
[32] Tian X, Wang F, Luo Y, Ma S, Zhang N, Sun Y, You C, Tang G, Li S, Gong Y and Xie C. Protective role of nuclear factor-erythroid 2-related factor 2 against radiation-induced lung injury and inflammation. Front Oncol 2018; 8: 542.
[33] Slezak J, Kura B, Babal P, Barancik M, Ferko M, Frimmel K, Kalocayova B, Kukreja RC, Lazou A, Mezesova L, Okruhlicova L, Ravingerova T, Singal PK, Szeiffova Bacova B, Viczenczova C, Vrbjar N and Tribulova N. Potencial markers and metabolic processes involved in mechanism of radiation-induced heart injury. Can J Physiol Pharmacol 2017; 95: 1190-1203.
[34] Fajardo LF and Stewart JR. Experimental radiation-induced heart disease. I. Light microscopic studies. Am J Pathol 1970; 59: 299-316.